OLD DOMINION UNIVERSITY RESEARCH FOUNDATION

DEPARTMENT OF PHYSICS
SCHOOL OF SCIENCES AND HEALTH PROFESSIONS
OLD DOMINION UNIVERSITY
NORFOLK, VIRGINIA

Technical Report PTR-81-9

THEORETICAL STUDIES OF SOLAR-PUMPED LASERS

By

Wynford L. Harries, Principal Investigator

Progress Report
For the period January 15, - July 15, 1981

Prepared for the
National Aeronautics and Space Administration
Langley Research Foundation
Hampton, Virginia

Under
Research Grant NSG 1568
John Wilson, Technical Monitor
Space Systems Division

August 1981

DEPARTMENT OF PHYSICS
SCHOOL OF SCIENCES AND HEALTH PROFESSIONS
OLD DOMINION UNIVERSITY
NORFOLK, VIRGINIA

Technical Report PTR-81-9

THEORETICAL STUDIES OF SOLAR-PUMPED LASERS

By

Wynford L. Harries, Principal Investigator

Progress Report
For the period January 15, - July 15, 1981

Prepared for the
National Aeronautics and Space Administration
Langley Research Foundation
Hampton, Virginia 23665

Under
Research Grant NSG 1568
John Wilson, Technical Monitor
Space Systems Division

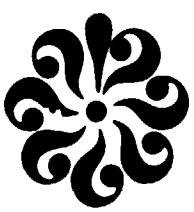

Submitted by the
Old Dominion University Research Foundation
P.O. Box 6369
Norfolk, Virginia 23508

August 1981

TABLE OF CONTENTS

LIST OF TABLES

LIST OF FIGURES

THEORETICAL STUDIES OF SOLAR-PUMPED LASERS

By

Wynford L. Harries*

SUMMARY

Estimates of the absorption and emission characteristics of molecules are required to predict new materials for solar-pumped lasers. These characteristics can be described in terms of the Franck Condon factors, which are calculated from the molecular wave functions.

Wave functions for vibrational levels in the lower and upper electronic states of I_2 and NSe are calculated numerically and methods of checking errors discussed. Errors arise when the vibrational quantum numbers are high; but, using a calculated rather than measured value of the dissociation energy, wave functions up to the fiftieth vibrational level are obtained. A new numerical method of evaluating the wave functions is given, which should be more accurate in the region of electronic transitions during absorption. Franck Condon factors, plotted versus the wavelength of the absorbed photons, are shown, and a check on the Franck Condon factors is made using the vibrational sum rule.

INTRODUCTION

In order to predict the performance of solar-pumped lasers as power converters, a knowledge of the absorption and emission characteristics of molecular materials is required. The data on several thousand diatomic molecules have been tabulated by Herzberg (ref. 1) and Huber and Herzberg (ref. 2). The information, where complete, yields the potential energy curves and vibrational levels of the molecules. The molecular wave functions can then be calculated and the Franck Condon factors obtained, which give information on the absorption and emission characteristics. The

*Professor, Department of Physics, Old Dominion University, Norfolk, Virginia 23508-0369

calculation of the wave functions is outlined in the next section, "Molecular Functions," which includes a discussion of the errors and methods of checking them. A new numeric method of calculating the wave functions using an asymptotic solution is also presented. There are many advantages to this new approach, including greater accuracy in calculating the probability of electronic transitions. Under the subsection titled "Franck Condon Factors," the Franck Condon factors are obtained from the wave functions and are calculated for a given lower and upper level. The energy difference between lower and upper levels corresponds to the wavelength λ of the absorbed photon; for a given lower and a series of upper levels, the Franck Condon factors are calculated and plotted vs. λ. The resulting curve is an approximate indication of the absorption cross section (per unit wavelength) vs. λ. The final sections of the text discuss conclusions and work to be performed.

MOLECULAR WAVE FUNCTIONS

Introduction

The molecular wave functions were first calculated following the method of Fazio (ref. 3). The wave functions are those of one atom of a biatomic molecular in a frame of reference whose origin is centered on the other atom. They are obtained as solutions of Schrodinger's equation in the radial form. The atom in question is assumed to be in a potential well $V(r)$ given by a Morse potential energy function (ref. 4):

$$V(r) = D_e \{1 - \exp [-\beta(r - r_1)]\}^2 \qquad (1)$$

where D_e is the dissociation energy, r_1 the equilibrium internuclear distance (fig. 1), and β is given by

$$\beta = \left(\frac{2\pi^2 c \mu}{h D_e}\right)^{1/2} \omega_e \qquad (2)$$

Here c is the velocity of light, μ is the reduced mass of the atom, h is the Planck constant, and ω_e is the harmonic molecular frequency. Substituting equation (1) into the Schrodinger equation yields

$$\frac{d^2\psi}{dr^2} + \frac{8\pi^2 \mu}{h^2}\left[E - D_e\left[1 - \exp\left[-\beta\left(r - r_1\right)\right]\right]^2\right]\psi = 0 \qquad (3)$$

The energy E is the eigenvalue for the anharmonic oscillator (ref. 3):

$$E(v) = hc\omega_e\left[\left(v + \frac{1}{2}\right) - \psi_e\left(v + \frac{1}{2}\right)^2 + y_e\left(v + \frac{1}{2}\right)^3\right] \qquad (4)$$

where ω_e is in cm^{-1} ($c\omega_e = \nu$, the frequency) and v is the vibrational quantum number. The first term is the solution for a harmonic oscillator, the last two arise because of the anharmonic nature of the Morse function.

The quantities μ, r_1, $\omega_e x_e$, $\omega_e y_e$ are available (refs. 1, 2) for many materials. For the lower level D_o, the energy difference between the ground vibrational state and the dissociation energy is given (fig. 1); hence,

$$D_e = D_o + \frac{1}{2} hc\omega_e$$

The value of $\omega_e y_e$ is sometimes included in reference 1 but not in reference 2.

For the upper electronic level, there exists another set of constants ω_e', $\omega_e x_e'$, $\omega_e y_e'$, and r_1'. Also given is the minimum energy of the upper curve T_e, but D_2 for the upper level (fig. 1) is calculated from

$$D_2 = \frac{(\omega_e')^2}{4\,\omega_e\, x_e'} \tag{5}$$

which assumes that $\omega_e yze' = 0$. Usually $\omega_e >> \omega_e x_e >> \omega_e y_e$ and $w_e' >> \omega_e x_e' >> \omega_e y_e'$ and for low values of equation (4) is accurate. For For $v > 10$ appreciable errors occur because the cubic term then becomes important.

The wave functions are obtained numerically (refs. 4-6). The value of E is given by equation (4) for a chosen v. The classical turning points of the potential well are then obtained from equation (1):

$$R_{\pm} = r_1 - \frac{1}{\beta} \log_e \left(1 \mp \sqrt{\frac{E(v)}{D_e}}\right) \tag{6}$$

For $r >> R_+$, the coefficient of ψ in equation (3) approaches a constant, and there is an asymptotic solution:

$$\psi \to \exp - \left[\sqrt{5.951 \times 10^{-2}\ \mu\ [V(r) - E)]}\ (r - r_1)\right] \tag{7}$$

and here

$$\frac{d\psi}{dr} \to \psi\, \frac{(\log_e \psi)}{(r - r_1)} \tag{8}$$

Substitution into the Schrodinger equation yields:

$$\frac{d^2\psi}{dr^2} = 5.951 \times 10^{-2}\ \mu\ (V(r) - E)\ \left(\psi + \frac{d\psi}{dr}\frac{dr}{2}\right) \qquad (9)$$

where dr is an increment towards the origin and negative. Values of ψ and $(d\psi/dr)$ at a distance dr closer to the origin are

$$\psi_2 = \psi + \frac{d\psi}{dr} + \frac{d^2\psi}{dr^2}\frac{dr}{2}\ dr \qquad (10)$$

and

$$\left(\frac{d\psi}{dr}\right)_2 = \frac{d\psi}{dr} + \frac{d^2\psi}{dr^2}\ dr \qquad (11)$$

The scheme proceeds iteratively to smaller r, and, as noted previously (ref. 4), the function diverges when $r < R_-$. By monitoring the signs of ψ and $d\psi/dr$, the computer recorded $\psi = 0$ when divergence occurred.

The normalized function obeys

$$\int_{-\infty}^{+\infty} \psi^2(r)\ dr = 1 \quad .$$

The values of ψ were stored, and ψ^2 integrated by Simpson's rule. Values were then obtained of the normalized function

$$\psi_N(r) = \frac{\psi_r}{\sqrt{\int_A^B \psi^2(r)\ dr}} \qquad (12)$$

where the limits A and B are chosen to satisfy an accuracy of five significant figures. The plots of ψ_N are superimposed onto the Morse curves (fig. 2). The position of the wave functions on the ordinate corresponds to the energy of the level, but their amplitudes are arbitrary although relative to each other. The reiteration scheme started for the lower curve at an upper limit of r such that $\psi \ll 10^{-49}$ and proceeded to a lower limit which was less than R_- in 2,490 increments. Every tenth value was stored for integration. For the lower level, the scheme started at r = 3.318 A and proceeded to 2.318 A. For the upper level, the integration was carried out in two parts: for the region from 5.051 to 3.318 A in 2,490 steps and from 3.318 to 2.318 A in 2,490 steps. The two regions were required for normalization, but the limits of r in the latter regions coincided with those of the lower level so that the integral of $\psi_v \psi_n$ could be evaluated when calculating the Franck Condon factor. Here n is the quantum number of the level in the upper electronic state.

Results for I_2

The curves in figure 2 are for I_2 with v = 0 and n = 45. The wave functions can be checked by counting the number of crossings of the axis (0 and 45). Tunneling at the limits is apparent, and plots of ψ^2_N showed that the probability of finding the atom at the turn around points in the upper level is about four times greater than at the center.

Although quantum numbers as high as 45 could be used for the upper level, for I_2 only $v \leq 10$ could be used for the lower level, otherwise too many crossing occurred. For v = 20 and 50, there were 21 and 57 crossings, respectively.

A second source of error occured for $r < R_-$ where the computer clamped the ψ_N to zero if it diverged. In figure 2(b), the wave functions do not approach zero asymptocically as $r \to -\infty$ in this section.

New Asymptotic Solution

The failure of the wave functions to approach zero asymptotically for r $\to -\infty$ occurs in the region where the Franck Condon factors are calculated. This region is susceptible to the accumulated errors of the reiterations. Attempts to use fewer steps were unsuccessful. Accordingly, an asymptotic solution for $\psi(r \to -\infty)$ was sought, with the view of carrying out a similar reiterative process with dr positive.

For $r \ll R_- < r_1$, the exponential term in equation (3) dominates and the equation takes the form

$$y'' - a^2 \exp(-2bx)\, y = 0 \tag{13}$$

where a,b are constants. By the transformation

$$z = e^{bx} \tag{14}$$

equation (13) becomes

$$y'' + \frac{1}{z} y' - \frac{a^2}{b^2} y = 0 \tag{15}$$

This is a form of Bessel's equation whose solution is

$$y = AI_o\left(\frac{az}{b}\right) + BK_o\left(\frac{az}{b}\right) \tag{16}$$

where A and B are constants determined by the boundary conditions, and I_o, K_o are modified Bessel functions of the first and second kind. For large z, I_o (a^2/b) increases, and we need $y \to 0$; hence, $A = 0$. The constant B is evaluated here by the normalization procedure. For large z, K_o has an asymptotic limit:

$$K_o\left(\frac{az}{b}\right) \to \sqrt{\frac{\pi b}{2az}} \exp\left(-\frac{az}{b}\right) \tag{17}$$

The asymptotic solution is

$$\psi = \sqrt{\frac{\pi\beta}{2A\,(r_1 - r)}} \cdot \exp\left[-\frac{A\,(r_1 - r)}{\beta}\right] \tag{18}$$

where $A = 5.951 \times 10^{-2}\ \mu\ De$ and

$$\frac{d\psi}{dr} = \psi\left[\frac{A}{\beta} + \frac{1}{2}\,(r_1 - r)\right] \tag{19}$$

Using equation (18), the initial value of r was estimated when $\psi = 10^{-20}$ and the reiteration process carried out as before in 2,490 steps with dr positive. The plots of ψ (fig. 3a) are for v = 0, 10, and 45. A comparison of the new method with the previous shows the two methods yield almost identical results between the classical turning points, but the new method gives values of ψ which approach zero asymptotically for $r < R_-$. For $r > R_+$, the new method gives diverging values of ψ as the program monitor was not applied here to make $\psi_N = 0$. With v = 10, the error in ψ near R_+ would only contribute to the normalization constant. However both methods gave a wave function which crossed the axis 50 times when v = 45.

Errors Using Higher Quantum Numbers

It can be seen that for the lower level, both asymptotic solutions yield functions which cross the axis too many times (fig. 3a), but the functions behave properly for the upper level (fig. 2a) up to n = 45. In these plots, values of $\omega_e y_e$ and $\omega_e y_e'$ were taken to be zero, as they were not included in reference 2. In the case of the upper level, D_2 was calculated from equation (5), which assumes $\omega_e y_e = 0$. On calculating D_e from $\omega_e^2/4\,\omega_e x_e$ for the lower level of I_2, the estimated value was 2.32 eV, whereas the given value was 1.54 eV. Using the value D_e = 2.32 eV for the lower level, the wave function for v = 50 crossed the axis 50 times (fig. 4). Evidently the value of $\omega_e y_e$ is important for high quantum numbers and it cannot be assumed zero.

A value of $\omega_e y_e = -8.95 \times 10^{-4}$ taken from reference 1 was tried, but again for v > 10, the wave functions misbehaved. Attempts were made to estimate $\omega_e y_e$, as the limiting value of E(v) from equation (4) for larger v should be equal to D_e. If $\omega_e y_e = 0$, then the limiting value is $D_e' = \omega_e^2/4\,\omega_e y_e$. Thus, from equation (4), $D_e - D_e' = \omega_e y_e\, v_D^3$ where v_D is the quantum number just when dissociation occurs, which is given (ref. 1) by

$$v_D = \frac{\omega_e}{2\,\omega_e x_e} \tag{20}$$

Hence

$$\omega_e y_e = \left(D_e - \frac{\omega_e^2}{4\,\omega_e x_e}\right)\left(\frac{\omega_e}{2\,\omega_e x_e}\right)^{-3} \tag{21}$$

Using the estimated value $\omega_e y_e = -0.00118$ for v = 15, the wave function crossed the axis 16 times, so the value is not sufficiently accurate.

Next $\omega_e y_e$ was estimated at the turning point for the level. For a given v, $E(v)$ was calculated assuming $\omega_e y_e = 0$, and the value of v at the turning point A (fig. 1) was calculated. The dotted curve is obtained assuming $D_e' = \omega_e^2/4\ \omega_e x_e$. The length AB should be the contribution of the cubic term in equation (4) and, for $v = 50$, AB was approximately 2,000 cm^{-1}; hence $\omega_e y_e = 0.01553$. The value of $E(v)$ was then recalculated, but the level was too low, and the wave function crossed the axis only 41 times. Hence this method also failed. Further study to estimate $\omega_e y_e$ at a point on the Morse curves corresponding to the exact quantum level in question is underway.

Orthogonality

One check of the accuracy of the wave functions is to check for orthogonality by evaluating the quantity ε:

$$\varepsilon = \int_{-\infty}^{+\infty} \psi_{N,v}\ \psi_{N,v'}\ dr \to 0 \qquad (22)$$

where v,v' are different vibrational quantum numbers for the same electronic state. The wave functions are plotted for I_2 for $0 \leq v \leq 30$ in figure 5. The integration range was fixed from $r = 3.318$ to $r = 2.300$ A. The upper limit of r was determined when ψ was just greater than 10^{-49} when $v = 0$. Even though, when $v = 30$, iteration started at a value of r where the asymptotic solution was doubtful, nevertheless the wave function appeared reasonable. The quantity ε which should be zero is shown in table 1. The values ranged from about 4×10^{-4} for the 0 to 1 case, but as v' became larger, ε became larger and, for the $v = 0$ to 10 case, ε was 6×10^{-3}. For adjacent levels, v to $v + 1$, $\varepsilon < 10^{-3}$ up to $v = 10$. The low values of ε imply that wave functions for $0 \leq v \leq 10$ should be trustworthy in the lower level of I_2.

Franck Condon Factors

Once the wave functions are known, the Franck Condon Factors, F, were obtained from

$$F = \left[\frac{\int_A^B \psi_v \psi_n \, dr}{\sqrt{\int_A^B \psi_v^2 \, dr} \sqrt{\int_A^C \psi_n^2 \, dr}} \right]^2 \qquad (23)$$

with the limits of integration A,B and A,C chosen where the wave functions were neligibly small. The integration was carried out over 249 points using Simspon's rule. Values for the transitions from v = 0, 1, ... 10 to n = 0 to 25 were obtained for NSe. The values for the v = 0 level are given in table 2. The energy difference between the lower and upper levels was expressed in terms of the wavelength of the absorbed photon, and hence plots of F vs. λ were obtained.

The vibrational levels in the lower electronic level are fairly widely spaced, and the relative populations obey Boltzmann Statistics $N_v/N_o = \exp[-(E_v - E_o)/kT$. The fractions N_v/N_o denoted by Q_1 for T = 300 K and Q_2 for T = 1,000 K are given in table 3. Multiplying by Q_1 and Q_2 is equivalent to giving a statistical weight to the contribution of the various v levels in any absorption process. The Franck Condon factors multiplied by Q_1 and Q_2 for NSe are plotted as if they were a continuous function of wavelength λ in figures 6(a) and (b). The peak values of F are about the same for v = 0 to 10, but on multiplying by Q_1, Q_2 it can be seen that the contributions from the lower vibrational levels are the most important.

In the case of I_2, it has been shown that using the calculated rather than the measured value of D_e gives different values to E and F (tables 1 and 4). The values of F for the two cases are compared for v = 0 in figure 7 and the differences are small. The differences would be greater for higher v. In figures 8 and 9, plots are shown for I_2 for v = 0 to 5 to the n = 0 to 45 levels assuming D_e = 2.3226 eV. The lower vibrational levels are much more closely spaced and the broadening at 1,000 K is more evident.

Plots proportional to the absorption cross section per unit wavelength σ_a can be obtained from figures 6, 8, and 9 by multiplying F by the frequency v:

$$\sigma_a \propto vF \tag{24}$$

where v is the frequency of the absorbed photon and figures 6, 8, and 9 only roughly represent the absorption cross sections.

It should be emphasized that the selection rules have not been considered here. However, it can be seen that at 1,000 K the contributions from the higher v levels become more important; hence, the overall cross section, obtained by summing the individual contributions, shows a broadening, as observed experimentally for diatomic molecules. A more accurate calculation would result if F were multiplied instead by

$$\frac{\exp[-(E_v - E_o)/kT]}{\sum_{v=0}^{\infty} [\exp(-E_v - E_o)/kT]}$$

which is the true fraction out of the total population. In such a case the curves should not only broaden, but the peak value should also fall.

Vibrational Sum Rule

If the vibrational eigenfunctions are properly normalized, it can be shown from elementary properties of orthogonal functions that the sum of the squares of the overlap integrals (Franck Condon factors) summed over all values of the vibrational quantum numbers of the upper or of the lower states is equal to one (ref. 1):

$$\sum_{v}\left[\int_{-\infty}^{+\infty} \psi_v \, \psi_n \, dr\right]^2 = \sum_{n}\left[\int_{-\infty}^{+\infty} \psi_v \, \psi_n \, dr\right]^2 = 1 \qquad (25)$$

The values of the Franck Condon factors for I_2 are still appreciable at the limiting value of n = 45 (table 4). In the case of NSe, with v = 0 the range of n from 0 to 25 is sufficient for a summation, as contributions from higher n values would be small. The sum for NSe equals 0.858--slightly less than one.

CONCLUSIONS

Molecular wave functions have been calculated for several materials, and the methods can be applied in general. A new numeric asymptotic method of calculating wave functions is presented which gives greater accuracy in the region of interest for calculating Frank Condon factors; otherwise, the two methods agree almost exactly both in amplitude and wavelength. The wave functions for the vibrational levels, v,n (in the lower/upper electronic states, respectively) can be checked as they should cross the axis v and n times, respectively. For both methods of numerical calculation the results are accurate for $v < 10$ and work for n of at least 50 for I_2. The use of the orthogonality theorem gave a method of checking the accuracy of the wave functions. The reason for the failure in the lower electronic level is lack of information of the anharmonic coefficient $\omega_e y_e$, which was entered as zero. In the upper level the "dissociation" energy D_2 was calculated on the assumption $\omega_e y_e = 0$, and the vibrational levels E_n were exact. In contrast, in the lower electronic level, entering $\omega_e y_e$ as zero causes the $\omega_e y_e (v + 0.5)^3$ term to be neglected; and this becomes important at higher values of v.

In practice, estimates of the wave functions are adequate for the lower v levels because, at normal temperatures, high v levels are hardly

populated. Attempts to estimate better values of $\omega_e y_e$ were unsuccessful.

Plots were made of the Franck Condon factors plotted versus the wavelength of the absorbed photon, and the relative contribution from each of the lower v levels weighed with the population density. The resulting plots give an approximate representation of the absorption cross section per unit wavelength versus wavelength. Higher temperatures fill the upper v levels, resulting in broadening the absorption cross section, as observed experimentally. A check on the accuracy of the Franck Condon factors using the vibrational sum rule implied that the results were probably correct to within 20 percent for NSe.

FUTURE WORK

The present program, which uses an asymptotic solution at $r > R_+$, requires further work. Attempts to improve the accuracy of the wave functions at higher values of v should continue, by obtaining better estimates of $\omega_e y_e$ and E_v.

The method of solution, using the asymptotic value of ψ at $r < R_-$ (see "New Asymptotic Solution") should be further investigated. A minor modification is to monitor the values of ψ at $r > R_+$, and if divergence occurs as r increases, then ψ should be made either to decay exponentially (as it should) or else be clamped to zero.

The new mthod has a number of advantages. It should give more accurate values of ψ at $r < R_-$, the region of interest in the upper level for calculating Franck Condon factors. In addition, the wave functions at values of $E_n < T_e + D_2$ (fig. 1) should be investigated. These collisions would result in dissociation with one of the atoms in an excited state, the events of greatest interest in the solar laser program. The problem of normalization is now different, as the wave function is a

continuous wave as r increases to infinity. The possibility of "box" normalization arises (ref. 7).

In addition to dissociation probabilities for Morse curves, such as figure 1, where the upper level has a well, the possibility of calculating the transition to an upper level which is repulsive needs study. Repulsive curves can be represented by an exponential function asymptotically approaching D_e. Hence, the method described under "New Asymptotic Solution" would seem applicable.

The Franck Condon factors should be applied to estimate absorption and emission coefficients. The expressions for the coefficients can be considered to be in two parts, only one of which is given by the Franck Condon factor; the other part requires a knowledge of the dipole moments. Nevertheless, the Franck Condon factors give an indication of the peak absorption frequency and bandwidths.

The materials I_2 and NSe considered here were taken as examples of materials with closely and widely spaced vibrational levels, respectively. The programs should be applied to biatomic molecules which show promise for solar-pumped lasers. A list of possible candidates has been made already based on estimates of solar, kinetic, and quantum efficiencies.

ACKNOWLEDGMENTS

Useful discussions with P.M. Fazio of ODU and J.W. Wilson and W. Meador of NASA/LaRC are acknowledged. The author is grateful for the help given by Drs. J. Tweed and J.H. Heinbockel of the Department of Mathematical Sciences, Old Dominion University, in the solution of equation (13).

REFERENCES

1. Herzberg, G: Molecular Spectra and Molecular Structure. I. Spectra of Diatomic Molecules. VanNostrand Reinhold (N.Y.), 1950.

2. Huber, K.P.; and Herzberg, G.: Molecular Spectra and Molecular Structure. IV. Constants of Diatomic Molecules. VanNostrand Reinhold (N.Y.), 1979.

3. Fazio, P.M.: M.S. Thesis. Old Dominion University (Norfolk, Va.), May 1979.

4. Morse, P.M.: Phys. Review, Vol. 34, 1929, p. 57.

5. Rao, M.; and Copeland, G.: Franck Condon Factors. Virginia Academy of Science abstract, 1978.

6. Merrill, J.: Using Computers in Physics. Houghton Mifflin Co. (Boston), 1976.

7. Schiff, L.I.: Quantum Mechanics. 3rd Ed. McGraw Hill, p. 47.

Table 1. Check of orthogonality for the lower electronic state of I_2. (ε should be zero.)

v	v'	D_e = 1.54238 ev ε_1	D_e' = 2.3226 eV ε_2
0	1	5.31363E-04	4.52542E-04
0	2	-8.59353E-04	-1.20878E-04
0	3	-5.51362E-04	-1.12316E-03
0	4	2.35670E-03	1.86749E-04
0	5	-2.32164E-03	1.52555E-03
0	6	2.31647E-04	-1.38800E-03
0	7	2.76570E-03	-5.18621E-04
0	8	-5.09534E-03	2.30412E-03
0	9	5.55751E-03	-2.48984E-03
0	10	-4.33286E-03	1.01218E-03
0	11	1.38139E-03	1.36457E-03
0	12	3.80220E-03	-3.39540E-03
0	13	-1.02070E-02	4.30076E-03
0	14	1.96059E-02	-3.87695E-03
0	15	-2.03887E-02	2.30248E-03
0	16	1.61098E-02	2.11115E-04
0	17	-3.78880E-03	-2.98475E-03
0	18	-4.13057E-03	5.78928E-03
0	19	2.13110E-02	-8.11211E-03
0	20	-4.14329E-02	1.02149E-02
0	21	4.29821E-02	-1.12771E-02
0	22	-4.20040E-02	1.21616E-02
0	23	1.28654E-02	-1.23444E-02
0	24	-1.15173E-02	1.23976E-02
0	25	3.14628E-02	-1.20293E-02
0	26	-3.96282E-02	1.16603E-02
0	27	5.15905E-02	-1.10720E-02
0	28	-7.86934E-02	1.05751E-02
0	29	8.49150E-02	-1.00354E-02
0	30	-1.12780E-01	8.97976E-03
10	11	1.38139E-03	1.36457E-03
10	12	3.80220E-03	-3.39540E-03
10	13	-1.02070E-02	4.30076E-03
10	14	1.96059E-02	-3.87695E-03
10	15	-2.03887E-02	2.30248E-03

Table 2. Values of Franck Condon factors assuming transitions from v = 0 to the first 26 upper levels for NSe.

LOWER LEVEL 0 NO V= 0

UPPER LEVEL N	WAVELENGTH(A)	FRANCK-CONDON FACTOR
0	4.13205E+03	2.43943E-03
1	4.02436E+03	1.10533E-02
2	3.92388E+03	2.76614E-02
3	3.82994E+03	4.92627E-02
4	3.74198E+03	7.03649E-02
5	3.65947E+03	8.59509E-02
6	3.58197E+03	9.34244E-02
7	3.50908E+03	9.28440E-02
8	3.44043E+03	8.59406E-02
9	3.37569E+03	7.52319E-02
10	3.31459E+03	6.29275E-02
11	3.25685E+03	5.06936E-02
12	3.20225E+03	3.96852E-02
13	3.15057E+03	3.02724E-02
14	3.10162E+03	2.26549E-02
15	3.05521E+03	1.66658E-02
16	3.01120E+03	1.21274E-02
17	2.96943E+03	8.75237E-03
18	2.92977E+03	6.34492E-03
19	2.89210E+03	4.60472E-03
20	2.85631E+03	3.24604E-03
21	2.82229E+03	2.21126E-03
22	2.78994E+03	1.53926E-03
23	2.75919E+03	1.10463E-03
24	2.72995E+03	7.55805E-04
25	2.70215E+03	5.33192E-04

Table 3. Values of N_v/N_o for the lower electronic level of NSe at temperatures of 300 K--Q_1 and 1,000 K--Q_2.

V	Q1	Q2
0	1.00000E+00	1.00000E+00
1	1.07862E-02	2.57006E-01
2	1.16341E-04	6.60521E-02
3	1.25488E-06	1.69758E-02
4	1.35353E-08	4.36288E-03
5	1.45994E-10	1.12128E-03
6	1.57471E-12	2.88177E-04
7	1.69851E-14	7.40632E-05
8	1.83204E-16	1.90347E-05
9	1.97607E-18	4.89203E-06
10	2.13142E-20	1.25728E-06

Table 4. Franck Condon factors and wavelengths of absorbed photon for I_2 assuming (a) D_e = 2.3226 eV and (b) D_e = 1.54238 eV.

Upper Level N	Wavelength(a)	(a) D_e = 2.3226 eV	(b) D_e = 1.54238 eV
0	6.35907E+03	4.01147E-11	6.61321E-11
1	6.30925E+03	8.88556E-10	1.37305E-09
2	6.26081E+03	1.04896E-08	1.50448E-08
3	6.21369E+03	7.63628E-08	1.04427E-07
4	6.16786E+03	3.88813E-07	5.08900E-07
5	6.12327E+03	1.54644E-06	1.98076E-06
6	6.07989E+03	5.00328E-06	6.31746E-06
7	6.03767E+03	1.35183E-05	1.73429E-05
8	5.99659E+03	3.50995E-05	3.68480E-05
9	5.95660E+03	6.38936E-05	8.55731E-05
10	5.91768E+03	1.28567E-04	1.66596E-04
11	5.87979E+03	2.42982E-04	2.72807E-04
12	5.84290E+03	4.05475E-04	5.13571E-04
13	5.80699E+03	6.63928E-04	8.27440E-04
14	5.77205E+03	1.01771E-03	1.26836E-03
15	5.73799E+03	1.67700E-03	1.79648E-03
16	5.70485E+03	2.40271E-03	2.56311E-03
17	5.67257E+03	2.79847E-03	3.36568E-03
18	5.64115E+03	4.23408E-03	3.92146E-03
19	5.61056E+03	5.26100E-03	5.50430E-03
20	5.58077E+03	6.52957E-03	6.06752E-03
21	5.55176E+03	6.88834E-03	8.01665E-03
22	5.52353E+03	8.17924E-03	9.44802E-03
23	5.49604E+03	9.35455E-03	1.07569E-02
24	5.46927E+03	1.05341E-02	1.20727E-02
25	5.44322E+03	1.30689E-02	1.20319E-02
26	5.41787E+03	1.26405E-02	1.29187E-02
27	5.39320E+03	1.52894E-02	1.55352E-02
28	5.36919E+03	1.44727E-02	1.63759E-02
29	5.34583E+03	1.51307E-02	1.70611E-02
30	5.32310E+03	1.74582E-02	1.76543E-02
31	5.30100E+03	1.59885E-02	1.79767E-02
32	5.27950E+03	1.80716E-02	1.82278E-02
33	5.25860E+03	1.81786E-02	1.82741E-02
34	5.23829E+03	1.81219E-02	1.62976E-02
35	5.21855E+03	1.79284E-02	1.61512E-02
36	5.19937E+03	1.76884E-02	1.59519E-02
37	5.18074E+03	1.54734E-02	1.55115E-02
38	5.16265E+03	1.49269E-02	1.66757E-02
39	5.14509E+03	1.45221E-02	1.61740E-02
40	5.12805E+03	1.39850E-02	1.54611E-02
41	5.11152E+03	1.33407E-02	1.33317E-02
42	5.09550E+03	1.40920E-02	1.26653E-02
43	5.07997E+03	1.34094E-02	1.33826E-02
44	5.06492E+03	1.14654E-02	1.26248E-02
45	5.05036E+03	1.07847E-02	1.07436E-02
		0.376354	0.387588

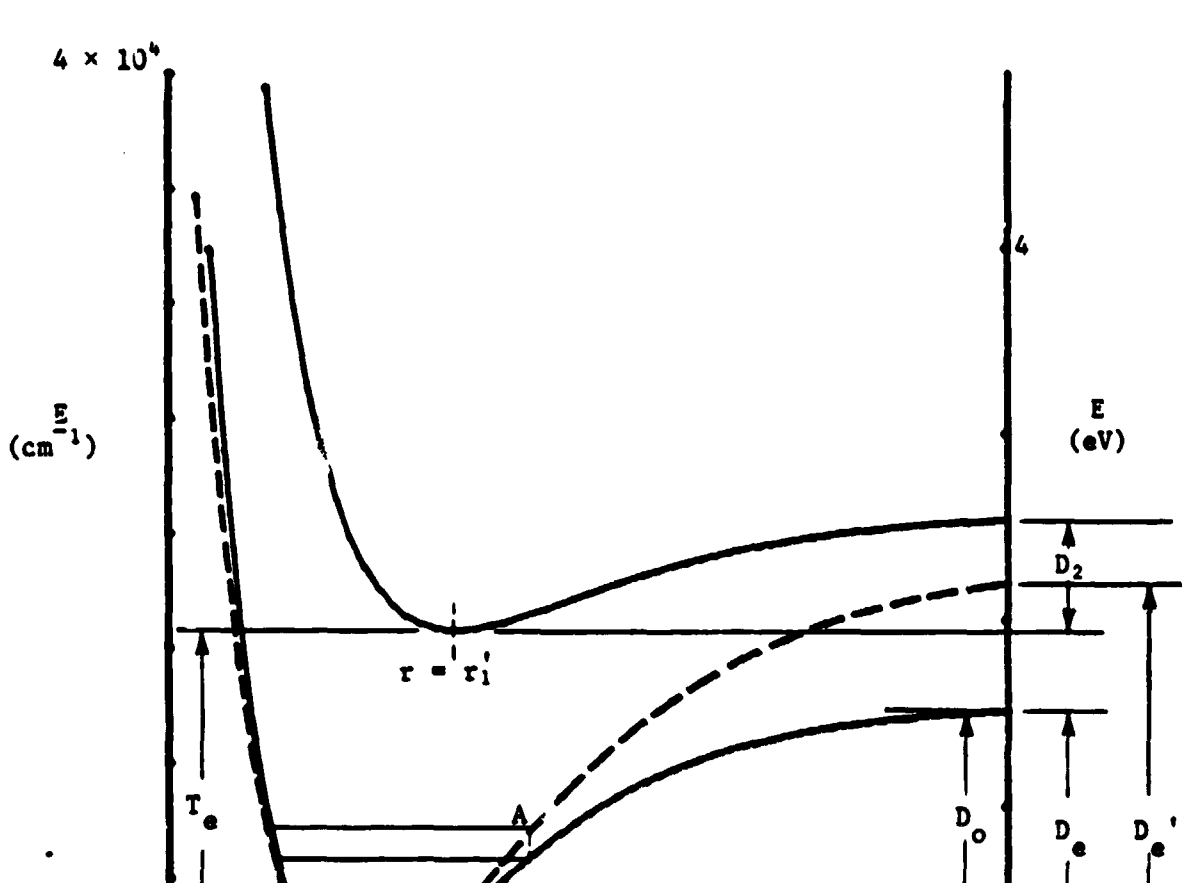

Figure 1. Examples of Morse curves for the ground state and the first electronically excited state of a biatomic molecule. The solid lower curve is calculated from the value of D_e in the literature. The dotted curve assumes $D_e' = \omega_e^2/4\,\omega_e x_e$.

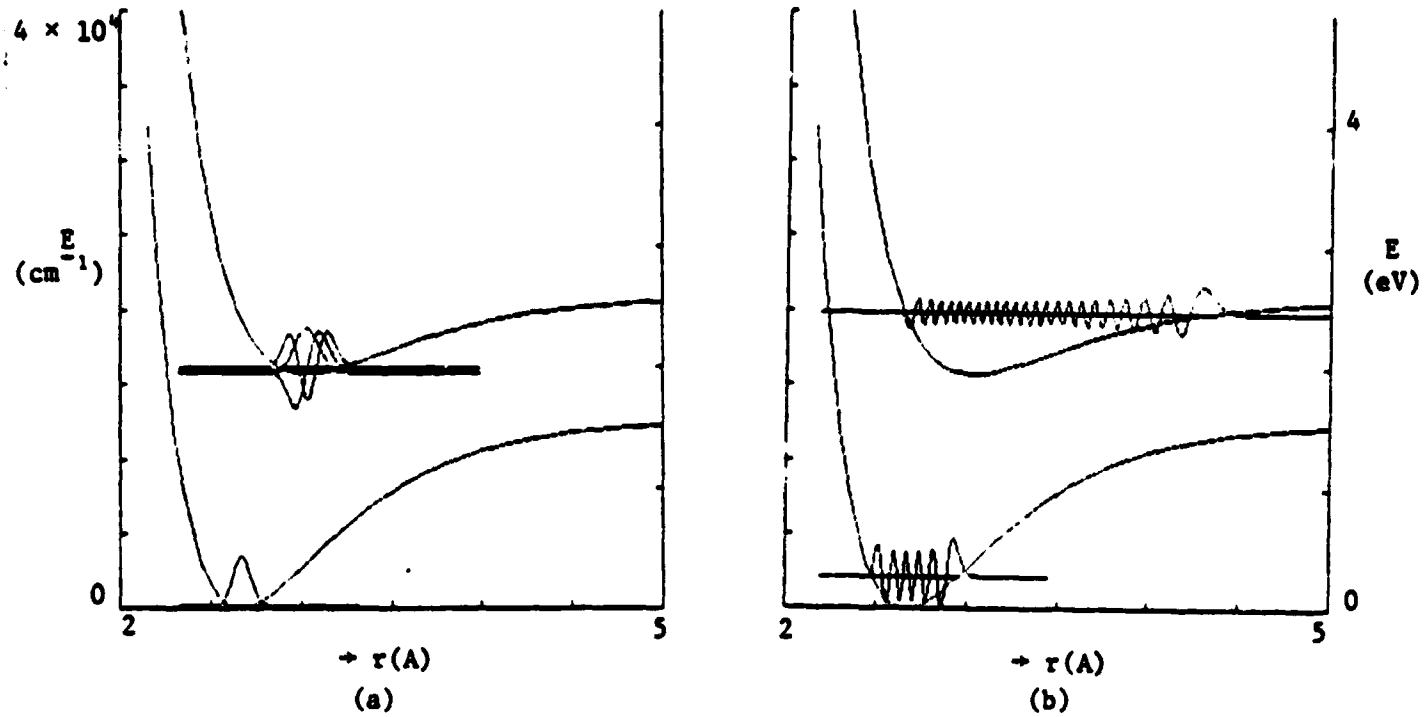

Figure 2. Morse curves for I_2: lower level $X^1 \Sigma_g^+$, upper level $B^3 \Pi_{o_u^+}$. The normalized wave functions (on an arbitrary vertical scale) are superimposed; (a) v = 0, n = 0,1,2; (b) v = 10, n = 45.

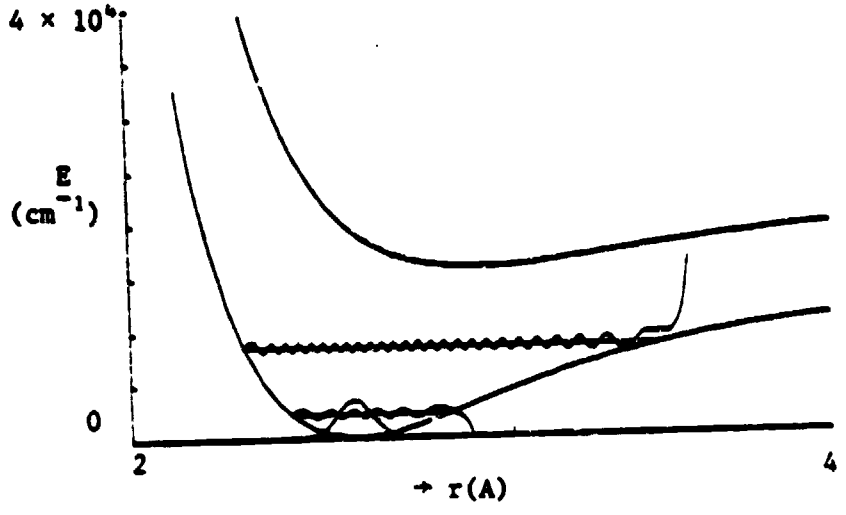

(a)

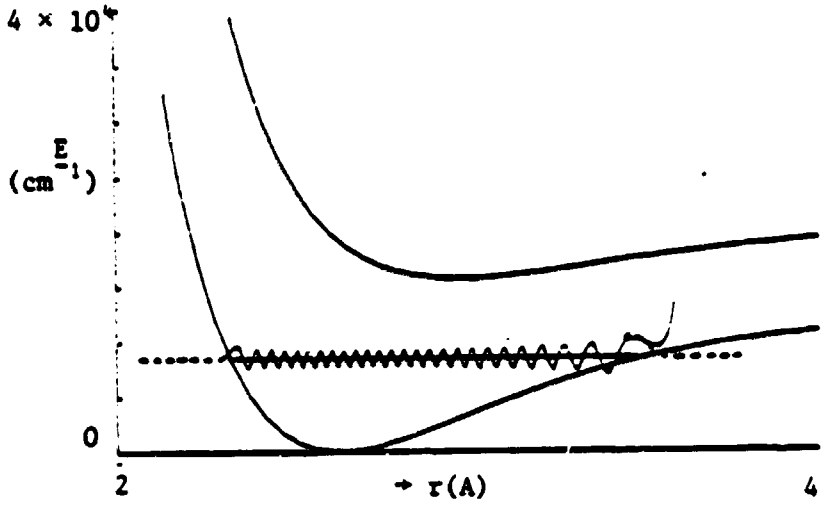

(b)

Figure 3. (a). Molecular wave functions for the lower electronic state I_2 using a new asymptotic method; (a) v = 0, 10, 45. (b). Comparison with previous asymptotic solution for v = 45 (continuous curve = new method; dotted curve = previous method).

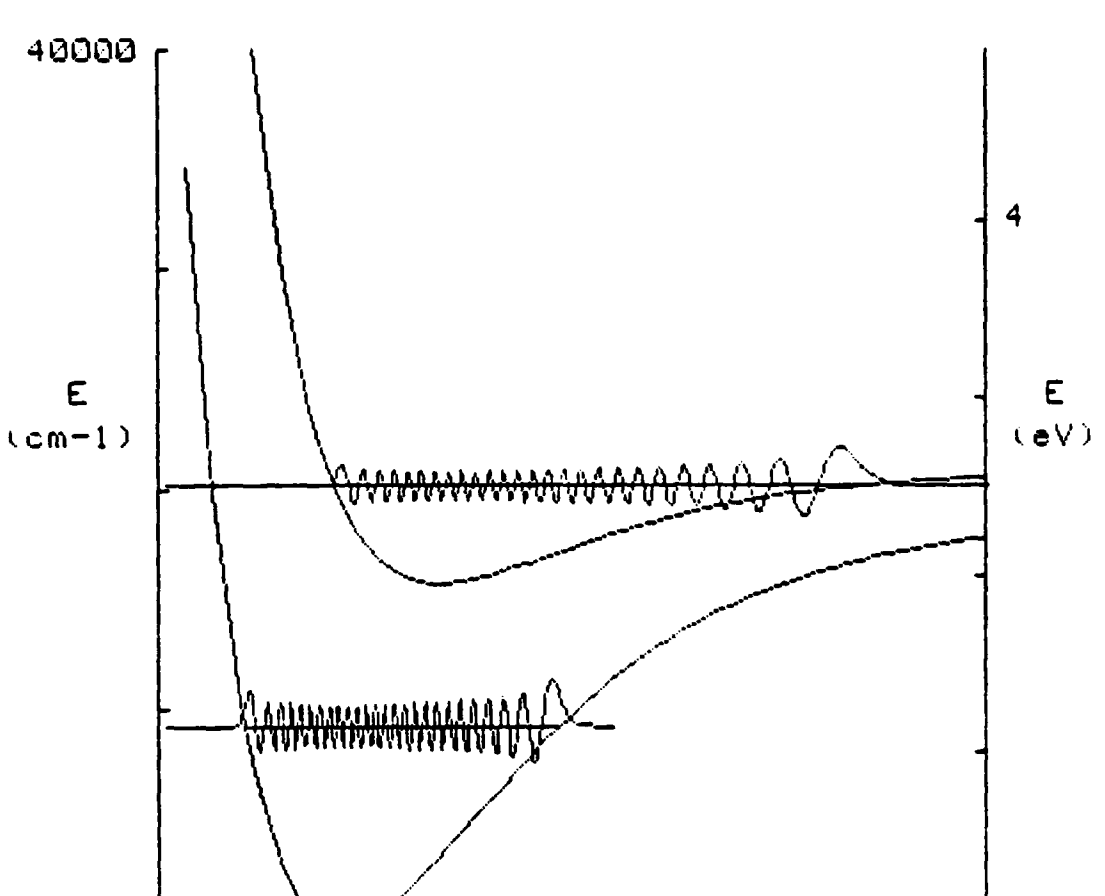

Figure 4. Morse curves for I_2: lower level X' Σ_g^+, upper level $B^3 \pi_g$ + v. The normalized wave functions for v, n = 50 are superimposed. Both cross the axis 50 times.

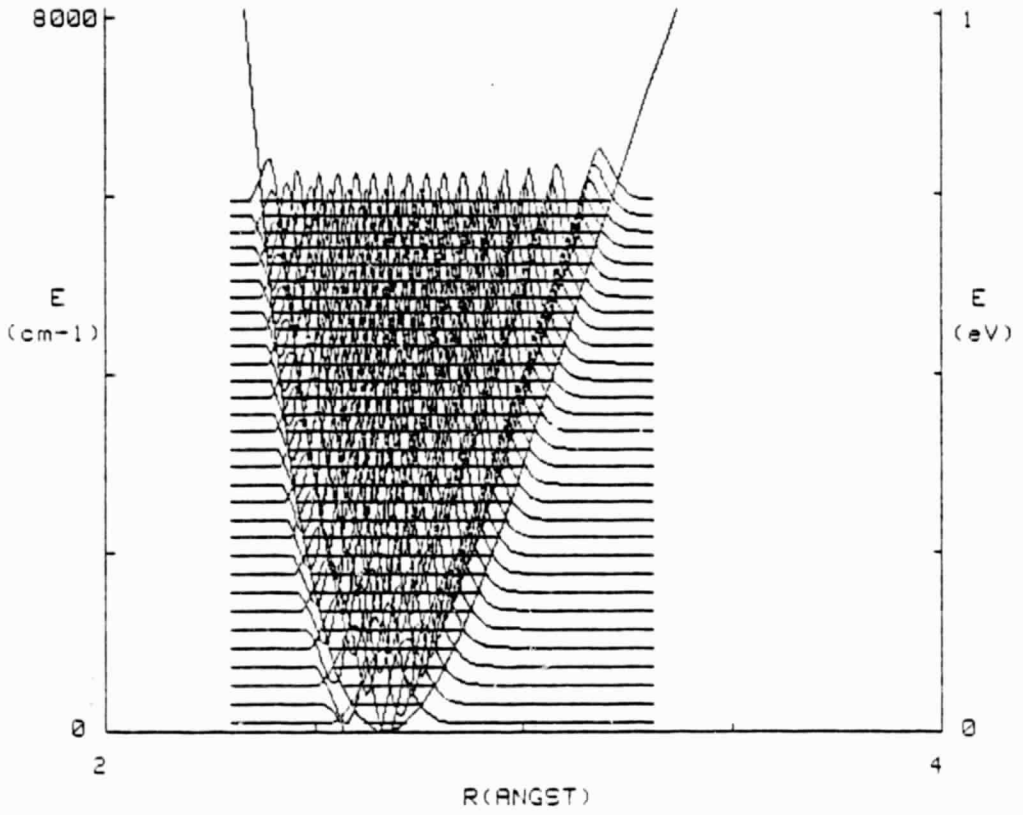

Figure 5. Test of orthogonality for the first 30 vibrational levels in the lower electronic level $X^1 \Sigma_q^+$ of I_2. $D_e = \omega_e^2/4\ \omega_e x_e = 2.3226$ eV.

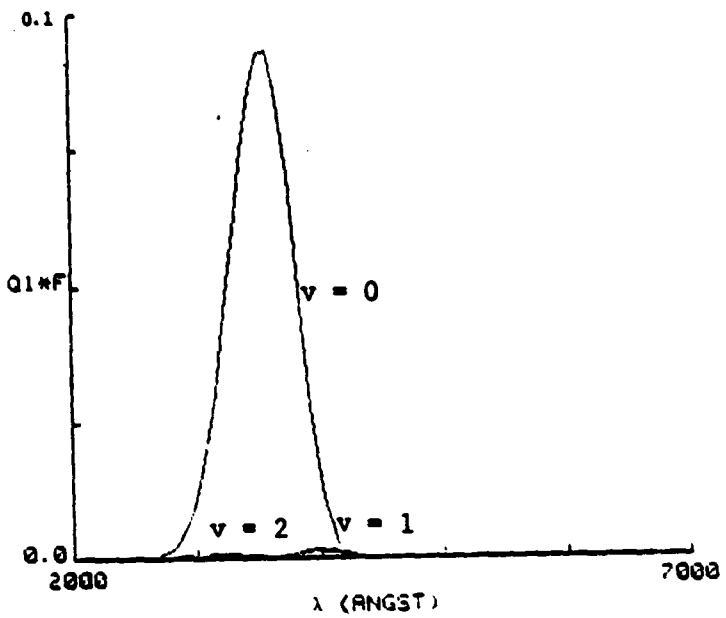

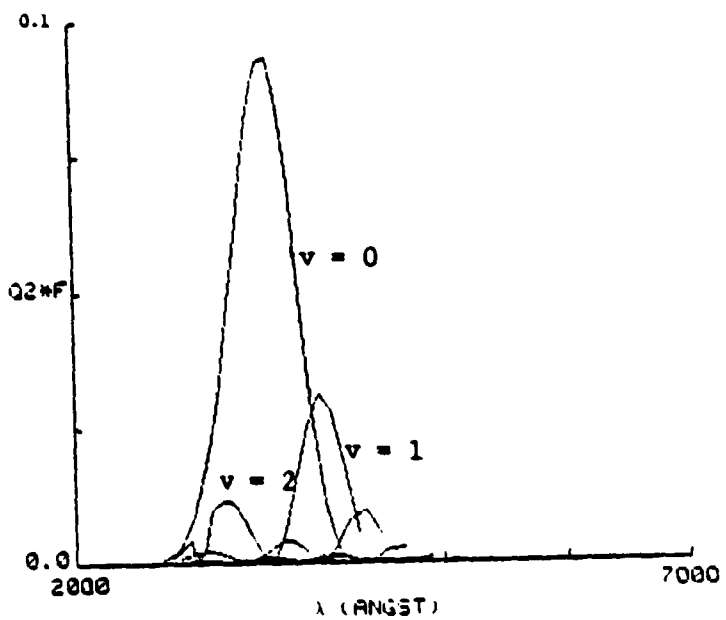

Figure 6. Plot of QF vs. wavelength for NSe (v = 0,1,2; n = 0 to 25) at temperatures of (a) 300 K and (b) 1,000 K.

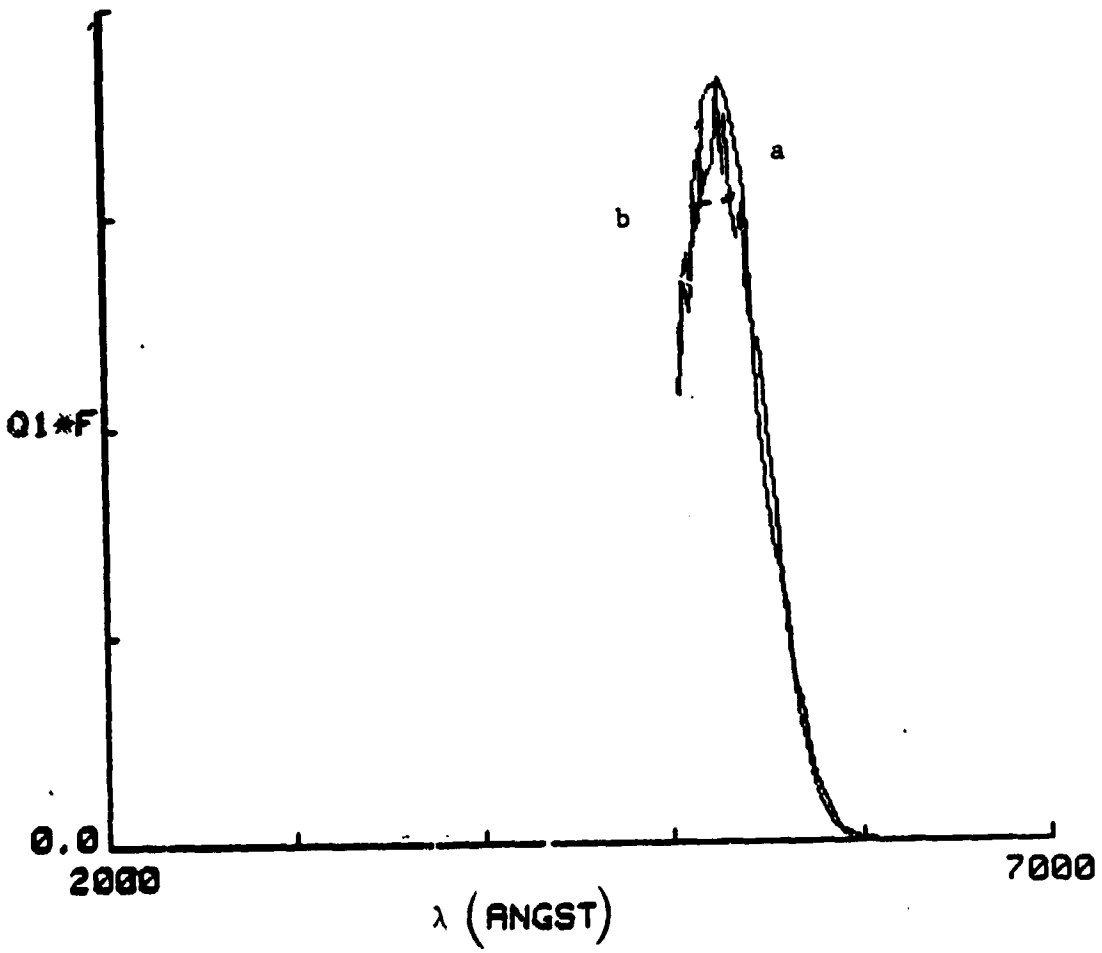

Figure 7. Plot of QF vs. wavelength of I_2 (v = 0; n = 0 to 45) for (a) D_e = 1.54238 eV, (b) D_e = 2.3226 eV.

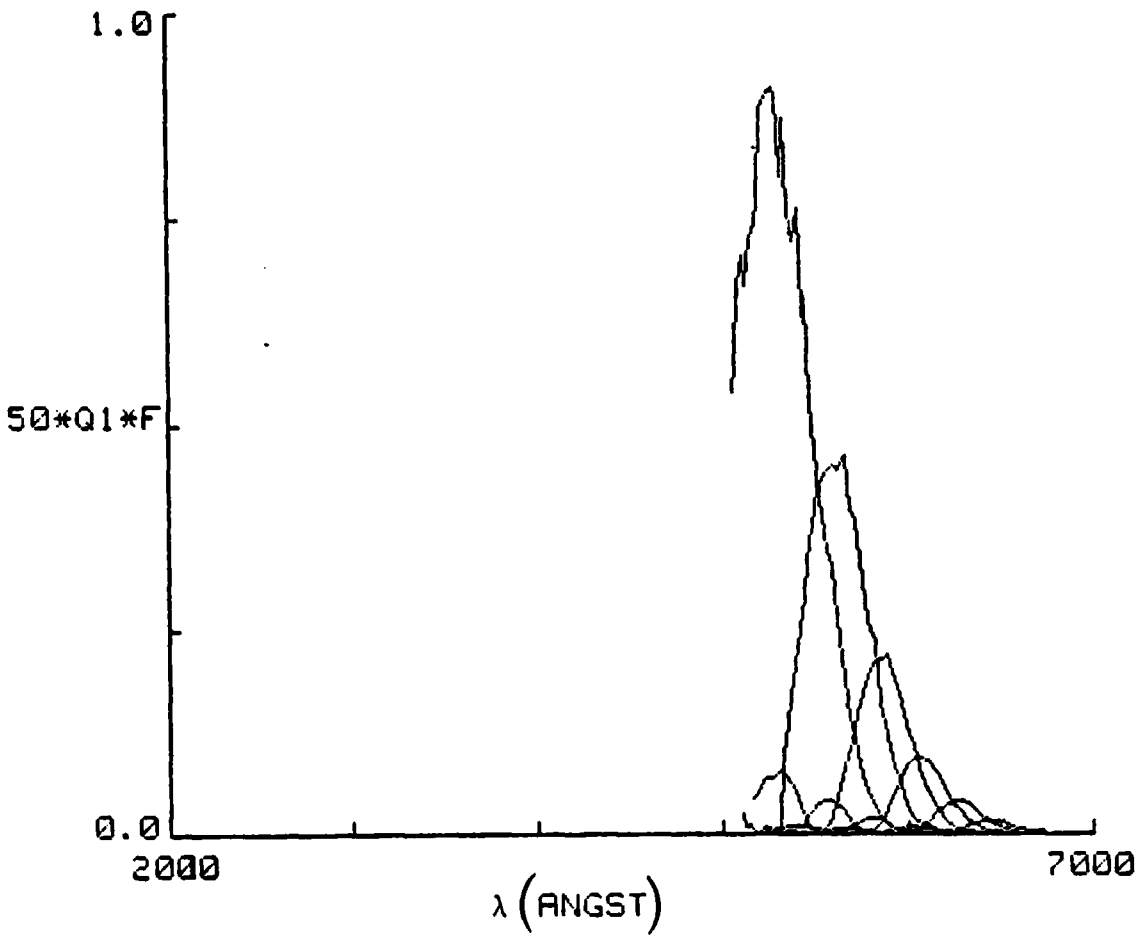

Figure 8. Plot of 50 QF vs. wavelength for I_2 (v = 0 to 5; n = 0 to 45; lower level $X^1 \Sigma_q^+$; upper level $B^3 \Pi_o + u$) at 300 K.

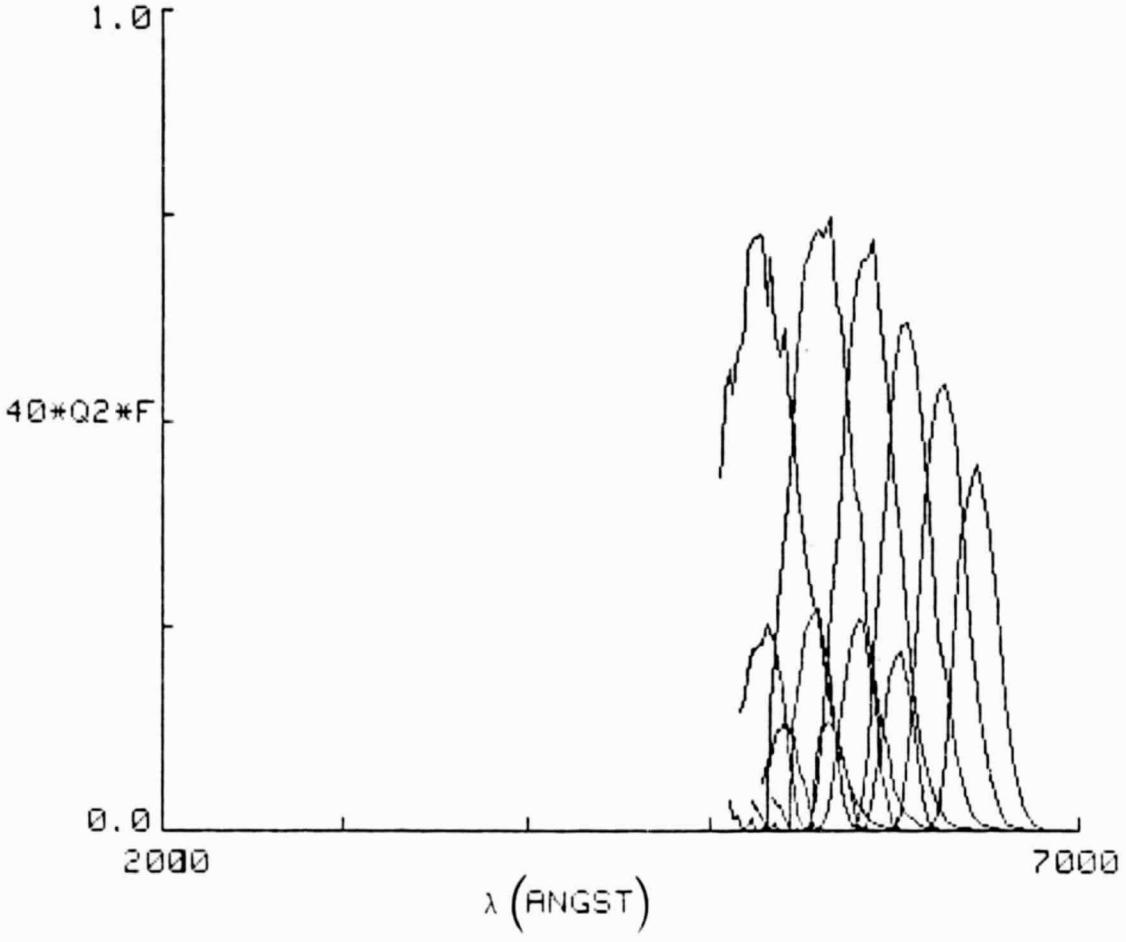

Figure 9. Plot of 40 QF vs. wavelength for I_2 (v = 0 to 5; n = 0 to 45; lower level $X^1 \Sigma_g^+$; upper level $B^3 \Pi_o + u$) at 1,000 K.